The unique effect of TDP-43 on hippocampal subfield morphometry and cognition

Ashley Heywood [a,*], Jane Stocks [a], Julie A. Schneider [b], Konstantinos Arfanakis [b,c], David A. Bennett [b], Mirza Faisal Beg [e], Lei Wang [a,d]

[a] Department of Psychiatry and Behavioral Sciences, Northwestern University Feinberg School of Medicine, Chicago, IL, USA
[b] Rush Alzheimer's Disease Center, Rush University Medical Center, Chicago, IL, USA
[c] Department of Biomedical Engineering, Illinois Institute of Technology, Chicago, IL, USA
[d] Department of Radiology, Northwestern University Feinberg School of Medicine, Chicago, IL, USA
[e] Simon Frasier University, Canada

1. Introduction

The relationship between neuropathologic disease and behavior is complex and poorly understood. It is well known that similar disease processes can present as a variety of clinical phenotypes. Conversely, similar clinical phenotypes can be caused by a variety of neuropathological disease processes. Even so, some older adults who maintained normal cognition during life have been found to have neuropathologic burden at autopsy. Therefore, the relationship between neuropathologic disease and brain functioning needs to be further explored. Alzheimer's disease (AD) is the most common cause of dementia (Alzheimer's Association, 2019), consisting of the characteristic amyloid-β and paired helical filament (PHF) tau tangle buildup in the brain. Non-AD pathologies such as vascular diseases, α-synucleinopathies, and transactive response DNA-binding protein of 43 kDA (TDP-43) proteinopathy have been interesting areas of research in recent years (Kovacs et al., 2013; Rahimi and Kovacs, 2014). While current biomarkers for amyloid-β and PHF-tau show promise for clinical utility (Klunk et al., 2004; Blennow et al., 2010; Craig-Schapiro et al., 2009; Gordon et al., 2016; Jack et al., 2013; Jack et al., 2010; Thal et al., 2006), current biomarkers for TDP-43 are insufficient. TDP-43 has been shown to be the primary proteinopathy involved in both amyotrophic lateral sclerosis (ALS) and frontotemporal lobar degeneration (FTLD) which causes the clinical syndromes of frontotemporal dementias (Neumann et al., 2006) and Limbic-predominant Age-related TDP-43 Encephalopathy (LATE; Nelson et al. 2019). Because of the wide array of neurodegenerative diseases that can contribute to multiple dementia syndromes, an early and accurate diagnosis of TDP-43 proteinopathy is crucial for the success of future therapeutic treatments.

Biomarkers for TDP-43 pathology have been studied with less success (Leuzy et al., 2019; Smith et al., 2019) than AD pathologic change. Additionally, the high specialization of PET, combined with minimally invasive lumbar puncture to gather cerebrospinal fluid, (Blennow, Vanmechelen, & Hampel, 2001; Mattsson & Zetterberg, 2009), perpetuates the challenge to develop non-invasive, readily available antemortem biomarkers for non-AD pathologic change. Structural MRI is a relatively non-invasive and readily available technique within the diagnostic workup for dementia syndromes, and can serve as an antemortem biomarker of postmortem disease (Bourgeat et al., 2010). The limbic system, and particularly the hippocampus, shows selective vulnerability to neurodegenerative disease accumulation. The hippocampus, and specifically its subfields, has been associated with unique functions both across the cytoarchitecturally distinct segments, and functional distinction along the long-axis, indicating specialization for anterior/posterior segmentations, due to their unique anatomical connections (de Wael et al., 2018). While most biomarker research surrounds hippocampal volumetry, hippocampal shape has been shown to be more sensitive in predicting disease progression in particular subfields in patients with dementia of the Alzheimer's type (DAT) as compared to controls (Csernansky et al., 2005; Wang et al., 2003) and studied in a variety of clinical groups (Cabinio et al., 2018; La Joie et al., 2013; Li et al., 2016; Wolf et al., 2001). While research has explored the relationship of hippocampal subfields to cognition, the literature is inconsistent (Xu et al. 2020; de Flores et al., 2015).

The goal of the present study was to identify *in-vivo* biomarkers of the TDP-43 disease process using hippocampal surface deformation based on high-dimensional structural MRI. In a previous study from our group, using the community-based studies (N = 42; average age at death = 90.4, SD = 5.0) we showed that shape deformity of the hippocampal CA1 and subiculum fields were uniquely associated with postmortem

---

amyloid-β burden across varying clinical diagnostic groups (Hanko et al., 2019), however, due to a small sample size, findings from TDP-43 were underpowered to be explored. The present study aimed to replicate these findings with an additional 57 subjects (total N = 99), and to further explore the role of the TDP-43 disease process in hippocampal surface deformation with greater power. We hypothesized that TDP-43 severity would be associated with a unique spatial pattern of hippocampal atrophy (Hanseeuw et al., 2019). Finally, we explored the relationship between morphology patterns and cognition to identify the unique effects of TDP-43 burden across several cognitive domains. We would expect deformation within unique subfields to be associated with specific cognitive impairments, as evidenced by previous research (Hanseeuw et al., 2011). Previous research has identified patients with pure LATE neuropathologic change (LATE-NC) showed a faster rate of cognitive decline within episodic memory and global cognition compared to participants without Alzheimer's disease neuropathologic change (ADNC) or LATE-NC. Patients with both ADNC and LATE-NC showed the fastest decline in episodic memory compared to either pathology alone and to subjects without pathologic change (Kapasi et al., 2020). Deformation associated with TDP-43 pathology is hypothesized to correlate to global cognition and episodic memory performance.

2. Methods and materials

2.1. Study population

Participants for the present study include a subset of participants from two longitudinal cohort studies at the Rush Alzheimer's Disease Center (RADC). The subset of subjects used in the current analysis are those who had undergone in vivo structural MRI before death and whose autopsy findings showed any sign of AD or TDP-43 pathology. The studies include the Religious Orders Study (ROS), which consisted of older Catholic nuns, priests, or brothers from across the United States, and the Rush Memory and Aging Project which consisted of older lay persons from across northeastern Illinois (MAP; Bennett et al., 2018). ROSMAP data can be requested at https://www.radc.rush.edu. The studies started in 1994 and 1997, respectfully. The sole inclusion criteria were being without known dementia and agreeing to annual clinical evaluation and organ donation; biennial MRI started in 2009 and was optional. Both studies were approved by an Institutional Review Board of Rush University Medical Center. All signed an informed consent, an Anatomical Gift Act for brain donation, and a repository consent to allow their data to be shared. Participants underwent annual detailed clinical evaluations including medical history, neurologic examination, and cognitive performance tests. Biennial MRI began in 2009. Cognitive impairment and dementia were determined by a 3-step process as previously reported (Bennett, et al., 2002). At the time of death, all available clinical data were reviewed by a neurologist with expertise in dementia, and a summary clinical diagnostic opinion was rendered regarding the most likely clinical diagnosis which was blind to all postmortem and imaging data including either no cognitive impairment (NCI), mild cognitive impairment (MCI), or Alzheimer's Dementia (AD). In cases which required adjudication, case conferences including one or more neurologists and a neuropsychologist were conducted to finalize a diagnosis. Diagnoses of dementia of the Alzheimer's type were made by a clinician and followed the recommendations of the National Institute of Neurological and Communicative Disorders and Stroke/Alzheimer's Disease and Related Disorders Association criteria (McKhann et al., 1984) and were consistent with the revised criteria (McKhann et al., 2011). A diagnosis of MCI referred to the presence of cognitive impairment in the absence of dementia, which is consistent with the most recent criteria (Albert et al., 2011).

2.2. Image acquisition, segmentation, and processing: Hippocampal surface plus subfield zone generation

Ante-mortem images were acquired on a 1.5 Tesla GE (General Electric, Waukesha, WI) MRI scanner, using a 3D magnetization-prepared rapid acquisition gradient echo (MPRAGE) sequence with the following parameters: Echo Time = 2.8 ms, Repetition Time = 6.3 ms, Field of View = 24 cm × 24 cm, flip angle = 8°, 160 slices, slice thickness of 1 mm, 224 ×192 image matrix, and 2 repetitions. To generate hippocampal segmentations, we used a previously designed pipeline: multi-atlas Freesurfer-Initiated Large Deformation Diffeomorphic Metric Mapping (FS-LDDMM; Christensen et al., 2015; Khan et al., 2008; Wang et al., 2009). FS-LDDMM is a fully automated procedure which consists of initial Freesurfer processing followed by LDDMM where a multi-atlas library of 74 scans containing expert manual segmentations of the hippocampus are initially aligned to the subject images based on high-dimensional transformations between each atlas and the subject. Voxel averaging the segmentations across the 74 atlas maps produces a final hippocampal segmentation for each subject. A tessellated template surface is injected into each subject's final hippocampal segmentation to create individual hippocampal surfaces that have vertex correspondence across subjects, consisting of 13, 222 vertices across left and right hippocampal surfaces, per subject. Visual inspection revealed no manual corrections were needed. We overlayed hippocampal subfield boundaries onto the surface to approximate subfield zones in order to aid in the interpretation of results.

2.3. Neuropathologic evaluation

Methods describing the neuropathologic evaluation have been described previously. Neuropathologic assessment follows gold-standard consensus recommendations following NIA Reagan criteria for the assessment of Alzheimer's disease and comorbid disease processes (Arvanitakis et al., 2011; Bennett et al., 2004; Dawe et al., 2011; Hyman & Trojanowski, 1997; Kotrotsou et al., 2015; Schneider et al., 2012; Schneider et al., 2004; Schneider et al., 2007; Braak and Braak, 1991), as summarized below:

At autopsy, left and right hemispheres of the deceased were removed and one hemisphere was immersion fixed in 4 % phosphate-buffered paraformaldehyde solution. The opposite hemisphere was subsequently cut into 1 cm thick coronal slabs and frozen. Hemispheric selection followed protocol including: (1) if significant pathology was identified in one hemisphere, fix that hemisphere, (2) if pathology was identified in both hemispheres, fix the more severely affected hemisphere, (3) if no observable pathology, fix the hemisphere with the lease mechanical damage during removal, (4) arbitrarily select the hemisphere for fixation if 1–3 did not apply. The cut and frozen slabs underwent tissue dissection and pathological diagnosis. The macro- and microscopic evaluation centered around the measurement of indices of both AD and coexisting neuropathological disease processes. A board-certified neuropathologist, blinded to age and clinical diagnosis, reviewed each case to assign a post mortem diagnosis based on a modified National Institute on Aging (NIA)-Reagan score for the presence and severity of AD neuropathologic change. This diagnosis relied on neurofibrillary tangles and plaques as guided by consensus recommendations (Bennett et al., 2006; Hyman and Trojanowski, 1997; Kotrotsou et al., 2015).

TDP-43 was assessed in five brain regions including the (1) amygdala, (2) hippocampus CA1, (3) hippocampus dentate gyrus, (4) entorhinal cortex, and (5) midfrontal cortex and were stained with monoclonal antibodies to phosphorylated TDP-43 (pS409/410; 1:100). A semi-quantitative rating of TDP-43 inclusions in a 0.25-mm^2 area of greatest density within that region was assigned as follows: none, sparse [1–2 inclusions], sparse to moderate [3–5 inclusions], moderate [6–12 inclusions], moderate to severe [13–19 inclusions], and severe [20 or more inclusions]. This semi-quantitative scoring procedure was

standardized such that severity scores are based on the same criteria for all subjects. An overall burden measure of TDP-43 pathology was created by summing the severity score in each region and dividing it by 5; this semi-quantitative overall burden score was used for analysis. While TDP-43 was only assessed in one hemi-sphere, previous research has identified that TDP-43 follows a bilateral deposition (Nelson et al., 2011), suggesting a non-lateralizing profile of TDP-43 in the hippo-campi. Therefore, we conclude that hemisphere selection is not shown to influence the pathology variables to be used in multivariate models for the manuscript.

Coexisting disease was measured for use as covariates in the present study including hippocampal sclerosis (HS), Lewy bodies, gross infarcts, atherosclerosis, arteriolosclerosis, and cerebral amyloid angiopathy (CAA). Coexisting disease pathology assessment can be seen in previously published works (Buchman et al., 2018; Kapasi et al., 2017). Lewy bodies were assessed using a monoclonal antibody to α-synuclein (Zymed LB 509; 1:50). A binary score indicating presence or absence of Lewy bodies was used in the present analysis. Gross and microscopic infarcts were scored as none (0), one (1), or more than one (2). Atherosclerosis, arteriosclerosis, and CAA were all rated on a 4-point scale from none to severe (0–3; Arvanitakis et al., 2017). Severity of atherosclerosis was graded by visual examination of the extent of involvement of each artery and number of arteries involved at the circle of Willis. Severity of arteriolosclerosis was assessed by the level of oc-clusion of vessels of the anterior basal ganglia (Arvanitakis et al., 2017; Kotrotsou et al., 2015). Severity of CAA (Boyle et al., 2015; Kotrotsou et al., 2015) was assessed and averaged across four regions: angular gyrus, midfrontal, temporal, and calcarine cortices.

2.4. Deformation and statistical analysis on surface

For each subject's hippocampal surface, perpendicular displace-ments from the population average were computed at each vertex which represented surface shape deformation. Statistical analysis on hippo-campal deformation at each vertex was performed using SurfStat in Matlab (Chung et al., 2010; Worsley et al., 2009). To investigate the relationship between hippocampal surface deformation and neuro-pathologic disease, multiple linear regression analysis was used. Multi-ple linear regression models were created using hippocampal surface deformation at each vertex as the dependent variable, resulting in 13,222 models for each subject. Our independent variable was TDP-43 severity. Covariates include age at death, sex, and time interval be-tween MRI and death. Coexisting diseases described above were also included as covariates with the exception of HS, as HS has been shown to truncate the variance associated with TDP-43 pathologic burden (Nelson et al., 2019). Additionally, to measure the unique effects TDP-43, we controlled for amyloid-β and PHF-tau overall burden. We produced two models of interest to present 1) the unique effect TDP-43 when con-trolling for demographic characteristics, and 2) the unique effect of TDP-43 when controlling for demographic characteristics and comorbid disease processes. These analyses were performed on the entire cohort (N = 99). Controlling for multiple comparisons was performed in the present study due to deformation at each vertex being necessarily correlated to neighboring vertices. Random Field Theory was applied utilizing a family-wise error rate of $p < 0.05$. Only the beta coefficients that remained significant after controlling for multiple comparisons were presented in the current work and were visualized as color-maps on the population hippocampal surface.

2.5. Association of pathologic deformation and cognition

We explored the relationship of *in-vivo* deformation due to TDP-43 and cognition. The following measures of cognition were used as pre-viously described (Bennett and Barnes, 2011): episodic memory, perceptual orientation, processing speed, semantic memory, working memory, and Mini-Mental State Exam (MMSE) score. Individuals' raw scores were converted to z-scores using the mean and standard deviation of the entire ROSMAP cohort at their baseline visit for each test. Z-scores from tests within each cognitive domain were averaged to create a composite z-score for each of the five domains. A measure of global cognition was calculated for each participant by averaging the z-scores from all 17 cognitive tests. In order to explore the relationship between the effects of TDP-43 disease burden on cognition, we (1) identified the vertices significantly related to TDP-43 from the most comprehensive model and (2) calculated an average deformation across those vertices for each subject. Deformation values were averaged across 1,901 sig-nificant vertices for TDP-43. Vertices were not bound by subfield boundaries, and instead represented all significant vertices which were identified from regression models. We then (3) calculated Pearson cor-relation coefficients between this average deformation and the cognitive z-scores.

3. Results

3.1. Ante-mortem population characteristics

Demographic information including age at the time of MRI scan, age at death, sex, and number of years of education, and clinical diagnosis at last study visit is provided in Table 1. Total average left hippocampal volume (standard deviation) was 1493 (207) and right 1687 (240) mm^3. Overall, subjects had a spectrum of ante-mortem clinical di-agnoses. Of the 99 subjects, 50 were determined to have no cognitive impairment (NCI), 28 had a clinical diagnosis of MCI, and 21 had probable AD. Time interval between MRI and death was not significantly associated with TDP-43 pathology (t = 0.87605, df = 97, p-value = 0.3832).

3.2. Distribution of neuropathologies across subjects.

The presence of various neuropathologic disease processes upon autopsy is summarized in Table 2. Nearly all brains at autopsy contained more than one neuropathology of amyloid-β, PHF tau, or TDP-43 (91.9 %) with 41.4 % of brains containing all three pathologies. The large majority (83.8 %) also had at least one non-AD neuropathology, including TDP-43 pathology (n = 47: 17, localized to amygdala; 20, extension to hippocampus and/or entorhinal cortex; 10, extension to the neocortex), Lewy body diseases (n = 21: 3, nigral predominant; 11, limbic type; 8, neocortical type), HS (n = 5), and cerebral infarctions (n = 27, one chronic infarction, regardless of size/location; n = 29, more than one, regardless of size/location). Coexisting cerebrovascular pa-thologies were also common, including CAA (n = 76), cerebral athero-sclerosis (n = 71: 50, mild; 19, moderate; 2, severe), and arteriolosclerosis (n = 60: 37, mild; 20, moderate; 3, severe). Amyloid-β exhibited a wide spread, distributed evenly across brain regions,

Table 1
Demographic information.

Characteristics	Value
N	99
Male, n (%)	35 (35.4 %)
Age at Visit, M (SD) Median [range]	88.1 (5.86) 91.3 [68.4,101]
Age at Death, M (SD) Median [range]	90.7 (5.87) 88.1 [71.7,104]
Years between last MRI and death, M (SD) Median [range]	2.57 (1.19) 2.54 [0.17, 5.11]
Years of Education, M (SD) Median [range]	15.4 (3.3) 15 [5,23]
Ante Mortem Clinical Diagnosis, n (%)	
NCI	50 (50.5 %)
MCI	28 (28.2 %)
AD	21 (21.2 %)

Table 2
Summary of neuropathologic findings at autopsy.

Characteristics	N (%)
PHF-tau	
Presence	98 (98.9 %)
Hippocampal	98 (98.9 %)
Amyloid-β	
Presence	88 (88.9 %)
Hippocampal	66 (66.7 %)
TDP-43	
Presence	45 (45.4 %)
Hippocampal	28 (28.3 %)
Lewy Bodies	21 (21.2 %)
Hippocampal sclerosis	5 (5.1 %)
Cerebral Amyloid Angiopathy	76 (76.8 %)
Atherosclerosis	
None	28 (28.3 %)
Mild	50 (50.5 %)
Moderate	20 (20.3 %)
Severe	3 (3.0 %)
Arteriolosclerosis	
None	39 (39.4 %)
Mild	37 (37.4 %)
Moderate	20 (20.2 %)
Severe	3 (3.0 %)
Chronic Infarcts (any size)	
None	43 (43.4 %)
One	27 (27.3 %)
Multi-infarct	29 (29.3 %)

whereas PHF-tau was more localized to the entorhinal cortex, hippocampus, and mesial temporal cortex. For TDP-43, the area most affected in subjects was the amygdala (41.4 %), followed by hippocampal CA1 (28.3 %), entorhinal cortex (24.2 %), and dentate gyrus (18.2 %).

3.3. Relationship between neuropathologic burden and hippocampal surface deformity

Results from the regression analysis in Fig. 1 show hippocampal surface maps representing the relationship between overall burden TDP-43 (average TDP-43 severity score across 5 brain regions) and hippocampal surface deformity for all 99 subjects after accounting for age, sex, and time between MRI and death (top row) and after additionally accounting for coexisting pathology (bottom row). More severe TDP-43 burden was associated with inward deformity in the surface zone approximating CA1. After accounting for the coexisting pathology, associations with each pathology demonstrate a distinct spatial pattern which recapitulate results from the first model which explored relationships without controlling for coexisting disease pathology. In an experiment not presented here, deformation patterns of amyloid-β and PHF-tau replicated previous findings from our group, and can be found in the supplemental materials (Hanko et al., 2019). Results of the model can be found in supplemental materials.

3.4. Relationship between neuropathologic burden associated hippocampal surface deformity and cognition

Correlations between TDP-43 associated hippocampal surface deformity and cognition can be seen in Table 3. Deformation associated with TDP-43 was significantly correlated to episodic memory perceptual orientation, processing speed, semantic memory, global cognition and MMSE score. Working memory was the only cognitive domain not associated with deformation related to TDP-43 pathologic burden.

4. Discussion

In the present analysis, we examined the effects of the TDP-43 disease process on hippocampal surface deformation. We utilized antemortem structural MRI imaging and postmortem neuropathological quantification. Results showed a deformation pattern unique to TDP-43 neuropathologic burden while controlling for coexisting disease processes. These results provide novel findings in addition to a previous experiment from our group (Hanko et al., 2019) in which TDP-43 relationships were not seen due to low power. The increased sample size in the present analysis allowed for enough power to detect the relationships between deformation and TDP-43 neuropathology after family-wise error correction. Critically, we also explored the effect of these deformation patterns on cognition in order to identify any unique clinical signatures of deformation due to disease. To our knowledge, this is the first study to explore such relationships to date.

TDP-43 burden, while controlling for the effects of amyloid-β and PHF-tau, was uniquely associated with inward deformation in bilateral CA1 and subiculum, and the most anterior portion of left hippocampus. After controlling for coexisting disease, the deformation pattern remains largely the same, with significant relationship between TDP-43 burden in bilateral subiculum and the left most anterior portion of the hippocampal head. These findings support previous research highlighting the medial temporal lobe to be susceptible to TDP-43 inclusions in AD (James et al., 2016; Josephs et al., 2014). Because of the unique deformation seen due to multi-region TDP-43 pathology, this deformation pattern could be a unique effect of the TDP-43 disease process on the selectively vulnerable hippocampal subfields. It is important to note these findings were seen only when hippocampal sclerosis (HS) was removed as a control variable from the model. It has been shown that HS is associated with severity of TDP-43 pathology (Nelson et al., 2019), and is proposed to be part of the spectrum of disease in Limbic-predominant Age-related TDP-43 Encephalopathy (LATE) neuropathologic changes. Therefore, controlling for HS truncates the variance associated with TDP-43 severity since we are tending to control for the most severe of TDP-cases. In an experiment not presented in the current paper, when HS was included in a multivariate model of the relationship between surface deformation and TDP-43 pathologic burden, there were no significant associations, thereby confirming this previous research. Recent studies have explored the role of TDP-43 in individuals with and without coexisting AD pathology (Josephs et al., 2017; Yu et al., 2020). Josephs et al. (2017) found that in a longitudinal study of patients with AD, hippocampal TDP-43 increased the rate of hippocampal atrophy when compared to patients without AD. Further Yu et al. (2020) found that TDP-43 and HS burden doubled the variance of hippocampal volume explained by AD pathology alone in patients with DAT but not in patients without DAT. This indicates that within Alzheimer's dementia patients, TDP-43 and HS pathology contribute to hippocampal atrophy above and beyond AD pathology alone. The findings additionally extend the research to show deformation within unique hippocampal subfields to be affected by TDP-43 pathology when accounting for AD pathology as well. Indeed, all individuals in the study with TDP-43 pathology, had some level of amyloid-β and tangles in their brain, supporting the role of TDP-43 in AD as a key mixed feature of the disease. Structural imaging research, which relies on hippocampal volume as an indicator of AD pathology without taking TDP-43 into consideration, could be missing key influence from the mixed disease state, and thus misinforming patient treatment and care.

The association of disease related burden on cognition was also explored in the present study. The study of regional differences within the hippocampus and their involvement in learning and memory has been explored from both a longitudinal-axis and transverse-axis perspective (Chen et al., 2010; Hrybouski et al., 2019; Nadel et al., 2013; Small, 2002; Strange et al., 2014). Previous research has indicated that the CA1 and subiculum are significantly associated with a variety of cognitive impairments (Lim et al., 2012A; Lim et al., 2012B).
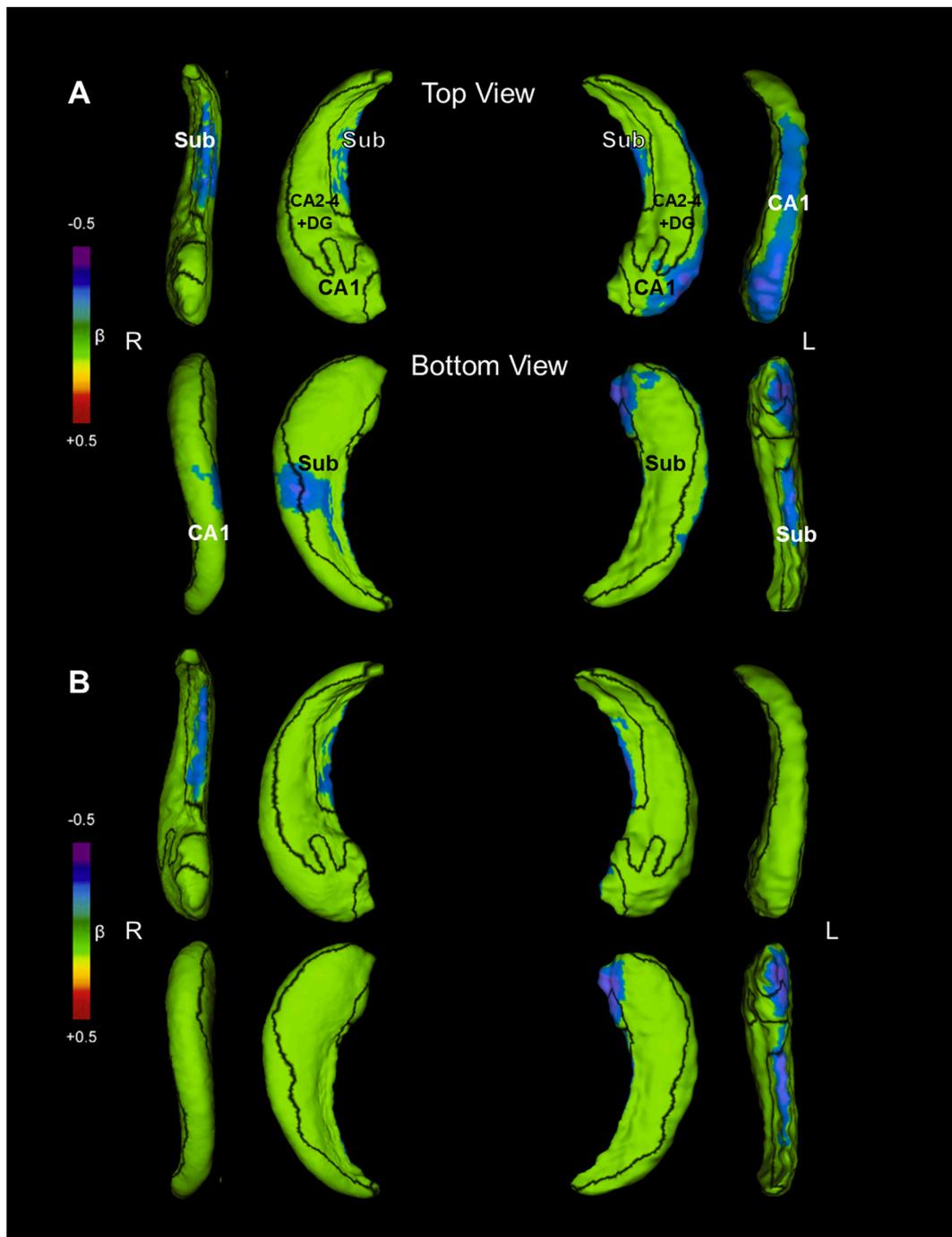
Fig. 1. Relationship between TDP-43 pathological burden and morphometry projected onto the hippocampal surface. Colors indicate strength of significant relationships between hippocampal surface deformations and pathology after correction for multiple comparisons. Cooler colors indicate a negative relationship, indicating an inward deformation. Black lines represent hippocampal subfield boundaries approximated on the hippocampal surface. A. The top rows show the results from a multivariate model controlling for amyloid-β, tau tangles, age, sex, and time between MRI and death. TDP-43 was uniquely associated with inward deformation in bilateral CA1 and subiculum, and the most anterior portion of left hippocampus. B. The bottom rows show the results from a multivariate model when additionally controlling for all other coexisting disease. After controlling for coexisting disease, the deformation pattern remains largely the same, with significant relationship between TDP-43 burden in bilateral subiculum and the most anterior portion of the left hippocampal head.

Specifically, in patients with probable AD, deformations within CA1 and subiculum were significantly correlated with verbal immediate, delayed, and recognition memory, in addition to constructional recall scores. The results from the present study support these findings as shown by deformation maps of TDP-43 burden (including CA1, subiculum, in addition to CA2-4) being significantly associated with semantic and episodic memory. Finally, the MMSE showed a significant relationship with TDP-43 morphometric burden which supports

previous research exploring hippocampal subfield volume across clinical diagnosis as determined by the MMSE (Mak et al., 2017). While the current research did find signification relationships of deformation and cognition, the results were non-specific to specific cognitive domains, that is, TDP-43 burden was associated with multi-domain cognitive impairment rather than focal cognitive deficits. This aligns with previous research noting the lack of specificity of hippocampal subfield volume relationships with current neuropsychological tests (de Wael et al.,

Table 3
Correlation between cognitive scores and pathologic related hippocampal deformation.

Cognition	Deformation due to TDP-43 burden
Episodic Memory	0.26**
Perceptual Orientation	0.26*
Processing Speed	0.22*
Semantic Memory	0.24**
Working Memory	n. s.
MMSE	0.39**
Global Cognition	0.30**

$*p < 0.05. **p < 0.01. ***p < 0.001.$

2018; Carmichael et al., 2012). Because of the cross-sectional and transdiagnostic nature of the present study, future research could explore the relationship of cognition and hippocampal deformation longitudinally to better understand the progression cognitive decline in relation to pathologic burden.

The results presented here add to the current literature by highlighting the utility of MRI as it relates to exploring the effect of postmortem TDP-43 disease burden on brain structure. There is great need for a non-invasive biomarker that is readily available in a general medical setting. Previous research has shown that hippocampal volume gathered from postmortem MRI is significantly associated with disease burden (Dawe et al., 2011; Van den Hauwe et al., 1995). Further, hippocampal atrophy from antemortem MRI was a fairly sensitive marker of the pathologic AD stage and cognitive status in a mixed clinical sample (Jack et al., 2002). As we have discussed above, PET imaging is a useful tool to measure amyloid concentrations in the brain, however, the clinical utility is limited due to its highly specialized nature (Ferreira and Busatto, 2011) and high costs (Medicare and Services). Further, the use of PET imaging for TDP-43 burden remains in developing research, further limiting is utility in identifying multiple coexisting diseases. And as mixed-dementias are now seen as the more common presentation compared to pure AD, the need for multiple PET scans only increases the burden of the patient. Therefore, these findings support previous literature and add a potential tool with high clinical utility to detect unique disease signatures in the *in-vivo* brain.

Strengths of our study include the use of postmortem neuropathologic assessment of TDP-43 disease burden. This is beneficial over relying on clinical diagnosis alone due to mixed disease states, as well as the poor correlation between clinical phenotypes and postmortem disease in some cases (Mesulam et al., 2014). Second, our study uses a single time point structural MRI which is beneficial over using several PET ligands for both patient burden and cost (de Leon et al., 2006). Next, our study utilizes a community sample of older adults which allows for greater generalizability of our research compared to studies which rely on recruitment from memory clinics alone. Further, utilizing cognitive assessment in this study allows for direct comparison of the deformation profiles and cognitive processes. This is crucial to further validate the deformation profiles as clinically relevant markers of cognitive decline. And finally, our sample size (N = 99) is large and allows for good power for the detection of differences within deformation profiles across diseases.

Our study also had several limitations. Firstly, the neuropathologic assessment for TDP-43 is a coarse measure of disease burden and future research is required for a finer assessment of pathology throughout the brain. Future research could address the quality and typing of TDP-43 inclusions to provide additional insight. This could impact our ability to detect deformation associated with disease and as such, results should be interpreted with caution. The lateralization pattern identified on deformation maps was unexpected and the authors propose this could be related to the hemisphere chosen for fixation (e.g., a larger proportion of samples could have been selected from the left-hemisphere). While the hemisphere selection was not available for review for the current analyses, the lateralization pattern could be an artifact of methodology or

could be due to left-sided vulnerability to neuropathologic disease. Validation and replication in other datasets could help answer this question. Another limitation is that our study population had a mean age of 88 years at the time of MRI, were highly educated, and a large portion were without cognitive impairment (50 %). Although a community sample allows for greater generalizability to the general population, this particular cohort of subjects may not represent a typical community sample. Memory clinics and community samples vary greatly in their demographics and disease burdens (Massoud et al., 1999), and, therefore, conclusions should be drawn with this in consideration.

CRediT authorship contribution statement

Ashley Heywood: Conceptualization, Investigation, Formal analysis, Methodology, Software, Visualization, Writing – original draft, Writing – review & editing. **Jane Stocks:** Writing – review & editing. **Julie A. Schneider:** Data curation, Funding acquisition, Writing – review & editing. **Konstantinos Arfanakis:** Data curation, Writing – review & editing. **David A. Bennett:** Data curation, Funding acquisition, Writing – review & editing. **Mirza Faisal Beg:** Writing – review & editing. **Lei Wang:** Conceptualization, Investigation, Funding acquisition, Supervision, Writing – review & editing.

Declaration of Competing Interest

The authors declare that they have no known competing financial interests or personal relationships that could have appeared to influence the work reported in this paper.

Data availability

The data used in this work can be made available upon request at www.radc.rush.edu

Appendix A. Supplementary data

Supplementary data to this article can be found online at https://doi.org/10.1016/j.nicl.2022.103125.

References

Albert, M.S., DeKosky, S.T., Dickson, D., Dubois, B., Feldman, H.H., Fox, N.C., Gamst, A., Holtzman, D.M., Jagust, W.J., Petersen, R.C., 2011. The diagnosis of mild cognitive impairment due to Alzheimer's disease: recommendations from the National Institute on Aging-Alzheimer's Association workgroups on diagnostic guidelines for Alzheimer's disease. Alzheimer's Dement 7 (3), 270–279.
Arvanitakis, Z., Leurgans, S.E., Wang, Z., Wilson, R.S., Bennett, D.A., Schneider, J.A., 2011. Cerebral amyloid angiopathy pathology and cognitive domains in older persons. Ann. Neurol. 69 (2), 320–327.
Arvanitakis, Z., Capuano, A.W., Leurgans, S.E., Buchman, A.S., Bennett, D.A., Schneider, J.A., 2017. The relationship of cerebral vessel pathology to brain microinfarcts. Brain Pathol. 27 (1), 77–85.
Association, A., 2019. 2019 Alzheimer's disease facts and figures. Alzheimer's Dement 15 (3), 321–387.
Bennett, D.A., Barnes, L.L., 2011. Datasets for special series on cognitive reserve. J. Int. Neuropsychol. Soc. 17 (4), 587–592.
Bennett, D.A., Wilson, R.S., Schneider, J.A., Evans, D.A., Beckett, L.A., Aggarwal, N.T., 2002. Bach, J Natural history of mild cognitive impairment in older persons. Neurology 59 (2), 198–205.
Bennett, D.A., Schneider, J.A., Wilson, R.S., Bienias, J.L., Arnold, S.E., 2004. Neurofibrillary tangles mediate the association of amyloid load with clinical Alzheimer disease and level of cognitive function. Arch. Neurol. 61 (3), 378–384.

Bennett, D.A., Schneider, J.A., Tang, Y., Arnold, S.E., Wilson, R.S., 2006. The effect of social networks on the relation between Alzheimer's disease pathology and level of cognitive function in old people: a longitudinal cohort study. Lancet Neurol. 5 (5), 406–412.

Bennett, D.A., Buchman, A.S., Boyle, P.A., Barnes, L.L., Wilson, R.S., Schneider, J.A., 2018. Religious orders study and rush memory and aging project. J. Alzheimer's Dis. 64 (s1). S161–S189.

Blennow, K., Vanmechelen, E., Hampel, H., 2001. CSF total tau, Aβ42 and phosphorylated tau protein as biomarkers for Alzheimer's disease. Mol. Neurobiol. 24 (1), 87–97.

Blennow, K., Hampel, H., Weiner, M., Zetterberg, H., 2010. Cerebrospinal fluid and plasma biomarkers in Alzheimer disease. Nat. Rev. Neurol. 6 (3), 131.

Bourgeat, P., Chetelat, G., Villemagne, V., Fripp, J., Raniga, P., Pike, K., Acosta, O., Szoeke, C., Ourselin, S., Ames, D., 2010. β-Amyloid burden in the temporal neocortex is related to hippocampal atrophy in elderly subjects without dementia. Neurology 74 (2), 121–127.

Boyle, P.A., Yu, L., Nag, S., Leurgans, S., Wilson, R.S., Bennett, D.A., Schneider, J.A., 2015. Cerebral amyloid angiopathy and cognitive outcomes in community-based older persons. Neurology 85 (22), 1930–1936.

Braak, H., Braak, E., 1991. Neuropathological stageing of Alzheimer-related changes. Acta Neuropathol. 82 (4), 239–259.

Buchman, A.S., Nag, S., Leurgans, S.E., Miller, J., VanderHorst, V.G., Bennett, D.A., Schneider, J.A., 2018. Spinal Lewy body pathology in older adults without an antemortem diagnosis of Parkinson's disease. Brain Pathol. 28 (4), 560–568.

Cabinio, M., Saresella, M., Piancone, F., LaRosa, F., Marventano, I., Guerini, F.R., Clerici, M., 2018. Association between hippocampal shape, neuroinflammation, and cognitive decline in Alzheimer's disease. J. Alzheimers Dis. 66 (3), 1131–1144.

Carmichael, O., Xie, J., Fletcher, E., Singh, B., DeCarli, C., 2012. Initiative AsDN. Localized hippocampus measures are associated with Alzheimer pathology and cognition independent of total hippocampal volume. Neurobiol. Aging 33 (6), 1124. e31–.e41.

Chen, K.H., Chuah, L.Y., Sim, S.K., Chee, M.W., 2010. Hippocampal region-specific contributions to memory performance in normal elderly. Brain Cogn. 72 (3), 400–407.

Christensen, A., Alpert, K., Rogalski, E., Cobia, D., Rao, J., Beg, M.F., Weintraub, S., Mesulam, M.-M., Wang, L., 2015. Hippocampal subfield surface deformity in nonsemantic primary progressive aphasia. Alzheimer's Dement 1 (1), 14–23.

Chung, M.K., Worsley, K.J., Nacewicz, B.M., Dalton, K.M., Davidson, R.J., 2010. General multivariate linear modeling of surface shapes using SurfStat. Neuroimage 53 (2), 491–505.

Craig-Schapiro, R., Fagan, A.M., Holtzman, D.M., 2009. Biomarkers of Alzheimer's disease. Neurobiol. Dis. 35 (2), 128–140.

Csernansky, J., Wang, L., Swank, J., Miller, J., Gado, M., McKeel, D., Miller, M., Morris, J., 2005. Preclinical detection of Alzheimer's disease: hippocampal shape and volume predict dementia onset in the elderly. Neuroimage 25 (3), 783–792.

Dawe, R.J., Bennett, D.A., Schneider, J.A., Arfanakis, K., 2011. Neuropathologic correlates of hippocampal atrophy in the elderly: a clinical, pathologic, postmortem MRI study. PLoS ONE 6 (10).

de Flores, R., La Joie, R., Chételat, G., 2015. Structural imaging of hippocampal subfields in healthy aging and Alzheimer's disease. Neuroscience 309, 29–50.

de Leon, M.J., DeSanti, S., Zinkowski, R., Mehta, P.D., Pratico, D., Segal, S., Rusinek, H., Li, J., Tsui, W., Saint Louis, L.A., Clark, C.M., Tarshish, C., Li, Y., Lair, L., Javier, E., Rich, K., Lesbre, P., Mosconi, L., Reisberg, B., Sadowski, M., DeBernadis, J.F., Kerkman, D.J., Hampel, H., Wahlund, L.O., Davies, P., 2006. Longitudinal CSF and MRI biomarkers improve the diagnosis of mild cognitive impairment. Neurobiol. Aging 27 (3), 394–401.

de Wael, R.V., Larivière, S., Caldairou, B., Hong, S.J., Margulies, D.S., Jefferies, E., Bernhardt, B.C., 2018. Anatomical and microstructural determinants of hippocampal subfield functional connectome embedding. Proc. Natl. Acad. Sci. 115 (40), 10154–10159.

Ferreira, L.K., Busatto, G.F., 2011. Neuroimaging in Alzheimer's disease: current role in clinical practice and potential future applications. Clinics (Sao Paulo) 66 (Suppl 1), 19–24.

Gordon, B.A., Blazey, T., Su, Y., Fagan, A.M., Holtzman, D.M., Morris, J.C., Benzinger, T. L.S., 2016. Longitudinal β-amyloid deposition and hippocampal volume in preclinical alzheimer disease and suspected non-alzheimer disease pathophysiology. JAMA Neurol. 73 (10), 1192–1200.

Hanko, V., Apple, A.C., Alpert, K.I., Warren, K.N., Schneider, J.A., Arfanakis, K., Bennett, D.A., Wang, L., 2019. In vivo hippocampal subfield shape related to TDP-43, amyloid beta, and tau pathologies. Neurobiol. Aging 74, 171–181.

Hanseeuw, B.J., Betensky, R.A., Jacobs, H.I., Schultz, A.P., Sepulcre, J., Becker, J.A., Cosio, D.M.O., Farrell, M., Quiroz, Y.T., Mormino, E.C., 2019. Association of amyloid and tau with cognition in preclinical Alzheimer disease: a longitudinal study. JAMA Neurol. 76 (8), 915–924.

Hanseeuw, B., Van Leemput, K., Kavec, M., Grandin, C., Seron, X., Ivanoiu, A., 2011. Mild cognitive impairment: differential atrophy in the hippocampal subfields. Am. J. Neuroradiol. 32 (9), 1658–1661.

Hrybouski, S., MacGillivray, M., Huang, Y., Madan, C.R., Carter, R., Seres, P., Malykhin, N.V., 2019. Involvement of hippocampal subfields and anterior-posterior subregions in encoding and retrieval of item, spatial, and associative memories: Longitudinal transverse axis. Neuroimage 191, 568–586.

Hyman, B.T., Trojanowski, J.Q., 1997. Consensus recommendations for the postmortem diagnosis of Alzheimer disease from the National Institute on Aging and the Reagan Institute Working Group on diagnostic criteria for the neuropathological assessment of Alzheimer disease. J. Neuropathol. Exp. Neurol. 56 (10), 1095–1097.

Jack, C., Dickson, D.W., Parisi, J.E., Xu, Y., Cha, R., O'brien, P., Edland, S., Smith, G., Boeve, B.F., Tangalos, E.G., 2002. Antemortem MRI findings correlate with hippocampal neuropathology in typical aging and dementia. Neurology 58 (5), 750–757.

Jack Jr, C.R., Knopman, D.S., Jagust, W.J., Shaw, L.M., Aisen, P.S., Weiner, M.W., Petersen, R.C., Trojanowski, J.Q., 2010. Hypothetical model of dynamic biomarkers of the Alzheimer's pathological cascade. Lancet Neurol. 9 (1), 119–128.

Jack Jr, C.R., Knopman, D.S., Jagust, W.J., Petersen, R.C., Weiner, M.W., Aisen, P.S., Shaw, L.M., Vemuri, P., Wiste, H.J., Weigand, S.D., 2013. Update on hypothetical model of Alzheimer's disease biomarkers. Lancet Neurol. 12 (2), 207.

James, B.D., Wilson, R.S., Boyle, P.A., Trojanowski, J.Q., Bennett, D.A., Schneider, J.A., 2016. TDP-43 stage, mixed pathologies, and clinical Alzheimer's-type dementia. Brain 139 (11), 2983–2993.

Josephs, K.A., Whitwell, J.L., Weigand, S.D., Murray, M.E., Tosakulwong, N., Liesinger, A.M., Petrucelli, L., Senjem, M.L., Knopman, D.S., Boeve, B.F., 2014. TDP-43 is a key player in the clinical features associated with Alzheimer's disease. Acta Neuropathol. 127 (6), 811–824.

Josephs, K.A., Dickson, D.W., Tosakulwong, N., Weigand, S.D., Murray, M.E., Petrucelli, L., Liesinger, A.M., Senjem, M.L., Spychalla, A.J., Knopman, D.S., 2017. Rates of hippocampal atrophy and presence of post-mortem TDP-43 in patients with Alzheimer's disease: a longitudinal retrospective study. Lancet Neurol. 16 (11), 917–924.

Kapasi, A., DeCarli, C., Schneider, J.A., 2017. Impact of multiple pathologies on the threshold for clinically overt dementia. Acta Neuropathol. 134 (2), 171–186.

Kapasi, A., Yu, L., Boyle, P.A., Barnes, L.L., Bennett, D.A., Schneider, J.A., 2020. Limbic-predominant age-related TDP-43 encephalopathy, ADNC pathology, and cognitive decline in aging. Neurology 95 (14) e1951 e62.

Khan, A.R., Wang, L., Beg, M.F., 2008. FreeSurfer-initiated fully-automated subcortical brain segmentation in MRI using large deformation diffeomorphic metric mapping. Neuroimage 41 (3), 735–746.

Klunk, W.E., Engler, H., Nordberg, A., Wang, Y., Blomqvist, G., Holt, D.P., Bergström, M., Savitcheva, I., Huang, G.F., Estrada, S., 2004. Imaging brain amyloid in Alzheimer's disease with Pittsburgh Compound-B. Ann. Neurol. 55 (3), 306–319.

Kotrotsou, A., Schneider, J.A., Bennett, D.A., Leurgans, S.E., Dawe, R.J., Boyle, P.A., Golak, T., Arfanakis, K., 2015. Neuropathologic correlates of regional brain volumes in a community cohort of older adults. Neurobiol. Aging 36 (10), 2798–2805.

Kovacs, G.G., Milenkovic, I., Wöhrer, A., Höftberger, R., Gelpi, E., Haberler, C., Hönigschnabl, S., Reiner-Concin, A., Heinzl, H., Jungwirth, S., 2013. Non-Alzheimer neurodegenerative pathologies and their combinations are more frequent than commonly believed in the elderly brain: a community-based autopsy series. Acta Neuropathol. 126 (3), 365–384.

La Joie, R., Perrotin, A., de La Sayette, V., Egret, S., Doeuvre, L., Belliard, S., Eustache, F., Desgranges, B., Chételat, G., 2013. Hippocampal subfield volumetry in mild cognitive impairment, Alzheimer's disease and semantic dementia. NeuroImage: Clinical 3, 155–162.

Leuzy, A., Chiotis, K., Lemoine, L., Gillberg, P.-G., Almkvist, O., Rodriguez-Vieitez, E., Nordberg, A., 2019. Tau PET imaging in neurodegenerative tauopathies—still a challenge. Mol. Psychiatry 24 (8), 1112–1134.

Li, X., Li, D., Li, Q., Li, Y., Li, K., Li, S., Han, Y., 2016. Hippocampal subfield volumetry in patients with subcortical vascular mild cognitive impairment. Sci. Rep. 6, 20873.

Lim, H.K., Hong, S.C., Jung, W.S., Ahn, K.J., Won, W.Y., Hahn, C., Kim, I.S., Lee, C.U., 2012A. Hippocampal shape and cognitive performance in amnestic mild cognitive impairment. NeuroReport 23 (6), 364–368.

Lim, H.K., Jung, W.S., Ahn, K.J., Won, W.Y., Hahn, C., Lee, S.Y., Kim, I., Lee, C.U., 2012B. Relationships between hippocampal shape and cognitive performances in drug-naïve patients with Alzheimer's disease. Neurosci. Lett. 516 (1), 124–129.

Mak, E., Gabel, S., Su, L., Williams, G.B., Arnold, R., Passamonti, L., Rodríguez, P.V., Surendranathan, A., Bevan-Jones, W.R., Rowe, J.B., 2017. Multi-modal MRI investigation of volumetric and microstructural changes in the hippocampus and its subfields in mild cognitive impairment, Alzheimer's disease, and dementia with Lewy bodies. Int. Psychogeriatr. 29 (4), 545–555.

Massoud, F., Devi, G., Stern, Y., Lawton, A., Goldman, J.E., Liu, Y., Chin, S.S., Mayeux, R., 1999. A clinicopathological comparison of community-based and clinic-based cohorts of patients with dementia. Arch of Neurol 56 (11), 1368–1373.

Mattsson, N., Zetterberg, H., 2009. Alzheimer's disease and CSF biomarkers: key challenges for broad clinical applications. Biomarkers Med. 3 (6), 735–737.

McKhann, G., Drachman, D., Folstein, M., Katzman, R., Price, D., Stadlan, E.M., 1984. Clinical diagnosis of Alzheimer's disease: report of the NINCDS-ADRDA work group under the auspices of department of health and human services task force on Alzheimer's disease. Neurology 34 (7), 939.

McKhann, G.M., Knopman, D.S., Chertkow, H., Hyman, B.T., Jack Jr, C.R., Kawas, C.H., Klunk, W.E., Koroshetz, W.J., Manly, J.J., Mayeux, R., 2011. The diagnosis of dementia due to Alzheimer's disease: recommendations from the National Institute on Aging-Alzheimer's Association workgroups on diagnostic guidelines for Alzheimer's disease. Alzheimer's Dement 7 (3), 263–269.

Medicare Cf, Services M. Decision Memo for Beta Amyloid Positron Emission Tomography in Dementia and Neurodegenerative Disease (CAG-00431N). September 27, 2013.

Mesulam, M.-M., Weintraub, S., Rogalski, E.J., Wieneke, C., Geula, C., Bigio, E.H., 2014. Asymmetry and heterogeneity of Alzheimer's and frontotemporal pathology in primary progressive aphasia. Brain 137 (4), 1176–1192.

Nadel, L., Hoscheidt, S., Ryan, L.R., 2013. Spatial cognition and the hippocampus: the anterior–posterior axis. J. Cogn. Neurosci. 25 (1), 22–28.

Nelson, P.T., Schmitt, F.A., Lin, Y., Abner, E.L., Jicha, G.A., Patel, E., Kryscio, R.J., 2011. Hippocampal sclerosis in advanced age: clinical and pathological features. Brain 134 (5), 1506–1518.

Nelson, P.T., Dickson, D.W., Trojanowski, J.Q., Jack, C.R., Boyle, P.A., Arfanakis, K., Rademakers, R., Alafuzoff, I., Attems, J., Brayne, C., 2019. Limbic-predominant age-related TDP-43 encephalopathy (LATE): consensus working group report. Brain 142 (6), 1503–1527.

Neumann, M., Sampathu, D.M., Kwong, L.K., Truax, A.C., Micsenyi, M.C., Chou, T.T., Bruce, J., Schuck, T., Grossman, M., Clark, C.M., 2006. Ubiquitinated TDP-43 in frontotemporal lobar degeneration and amyotrophic lateral sclerosis. Science 314 (5796), 130–133.

Rahimi, J., Kovacs, G.G., 2014. Prevalence of mixed pathologies in the aging brain. Alzheimer's Res. Ther. 6 (9), 82.

Schneider, J.A., Arvanitakis, Z., Bang, W., Bennett, D.A., 2007. Mixed brain pathologies account for most dementia cases in community-dwelling older persons. Neurology 69 (24), 2197–2204.

Schneider, J., Wilson, R., Bienias, J., Evans, D., Bennett, D., 2004. Cerebral infarctions and the likelihood of dementia from Alzheimer disease pathology. Neurology 62 (7), 1148–1155.

Schneider, J., Arvanitakis, Z., Yu, L., Boyle, P., Leurgans, S., Bennett, D., 2012. Cognitive impairment, decline and fluctuations in older community-dwelling subjects with Lewy bodies. Brain 135 (10), 3005–3014.

Small, S.A., 2002. The longitudinal axis of the hippocampal formation: its anatomy, circuitry, and role in cognitive function. Rev. Neurosci. 13 (2), 183–194.

Smith, R., Santillo, A., Waldö, M.L., Strandberg, O., Berron, D., Vestberg, S., van Westen, D., van Swieten, J., Honer, M., Hansson, O., 2019. 18 F-Flortaucipir in TDP-43 associated frontotemporal dementia. Sci. Rep. 9 (1), 1–10.

Strange, B.A., Witter, M.P., Lein, E.S., Moser, E.I., 2014. Functional organization of the hippocampal longitudinal axis. Nat. Rev. Neurosci. 15 (10), 655–669.

Thal, L.J., Kantarci, K., Reiman, E.M., Klunk, W.E., Weiner, M.W., Zetterberg, H., Galasko, D., Praticò, D., Griffin, S., Schenk, D., 2006. The role of biomarkers in clinical trials for Alzheimer disease. Alzheimer Dis and Assoc Disord 20 (1), 6.

Van den Hauwe, L., Parizel, P., Martin, J., Cras, P., De Deyn, P., De Schepper, A., 1995. Postmortem MRI of the brain with neuropathological correlation. Neuroradiol 37 (5), 343–349.

Wang, L., Swank, J.S., Glick, I.E., Gado, M.H., Miller, M.I., Morris, J.C., Csernansky, J.G., 2003. Changes in hippocampal volume and shape across time distinguish dementia of the Alzheimer type from healthy aging. Neuroimage 20 (2), 667–682.

Wang, L., Khan, A., Csernansky, J.G., Fischl, B., Miller, M.I., Morris, J.C., Beg, M.F., 2009. Fully-automated, multi-stage hippocampus mapping in very mild Alzheimer disease. Hippocampus 19 (6), 541–548.

Wolf, H., Grunwald, M., Kruggel, F., Riedel-Heller, S., Angerhöfer, S., Hojjatoleslami, A., Hensel, A., Arendt, T., Gertz, H.-J., 2001. Hippocampal volume discriminates between normal cognition; questionable and mild dementia in the elderly. Neurobiol. Aging 22 (2), 177–186.

Worsley, K.J., Taylor, J., Carbonell, F., Chung, M., Duerden, E., Bernhardt, B., Lyttelton, O., Boucher, M., Evans, A., 2009. A Matlab toolbox for the statistical analysis of univariate and multivariate surface and volumetric data using linear mixed effects models and random field theory. NeuroImage Organis. Hum. Brain Mapp. 2009 Ann. Meet. S102.

Xu, R., Hu, X., Jiang, X., Zhang, Y., Wang, J., Zeng, X., 2020. Longitudinal volume changes of hippocampal subfields and cognitive decline in Parkinson's disease. Quantit. Imag. Med. Surg. 10 (1), 220.

Yu, L., Boyle, P.A., Dawe, R.J., Bennett, D.A., Arfanakis, K., Schneider, J.A., 2020. Contribution of TDP and hippocampal sclerosis to hippocampal volume loss in older-old persons. Neurology 94 (2) e142-e52.